www.rericjournal.ait.ac.th

Investigation of Heat Transfer Enhancement in a Parabolic Trough Collector with a Modified Absorber

A. Kajavali*[1], B. Sivaraman* and N. Kulasekharan[+]

Abstract – Parabolic trough collectors are widely used as a solar energy recovery device, with the reflected concentrated solar energy focused mostly to a single cylindrical tube. Experiments are conducted on a single tube absorber and a newly designed modified absorber with an absorber plate and a linear array of water tubes to utilize the most of the irradiated heat. Three dimensional, conjugate computational fluid dynamic analyses was carried out using a commercial software Ansys Fluent to analyse both single tube and modified absorber designs. The results from the present computations show good agreement with that of the present experiments. The solar energy recovery efficiency of the modified absorber was found to be higher than the single tube, in the form of increased water temperature. The proposed modified absorber can be an effective alternate for the parabolic trough collector systems. The day average efficiency of the proposed modified absorber system was found to be 42.1% which is higher than the conventional single tube absorber systems presently in use.

Keywords – CFD, conjugate thermal, FRP, modified absorber, parabolic trough collector.

1. INTRODUCTION

Solar energy capturing or conversion technologies include solar heating, solar photovoltaic, solar thermal electricity and solar architecture, which can make considerable contributions to solving some of the most pressing problem of energy crisis the world now faces. Among several solar thermal energy conversion technologies, the concentrating solar collectors using reflectors have gained more importance due to the inherent benefits. Even in concentrating type of solar collectors, several issues were inherent like dust accumulation over reflector surfaces, inability to maintain the focal point and solar tracking system errors.

Parabolic trough collectors (PTC) are widely used as a solar energy recovery device, with the reflected concentrated solar energy focused to a single cylindrical tube that is positioned along the focal line of the trough. Sometimes a transparent glass tube envelops the receiver tube to reduce heat loss. Parabolic troughs often use single-axis or dual-axis tracking and in rare instances, they may be stationary. Temperatures at the receiver can reach 400°C and produce steam for generating electricity [1]. Starting with Ericsson [2], several researchers across the world have worked and elaborately reported experimental, theoretical and numerical analysis of PTC systems in open literature. Reviews like Spencer [3] and Garcia *et al.* [1] summarized the technology development in the solar thermal energy conversion and using parabolic trough collectors respectively.

Kalogirou [4] tested the collector's performance according to ASHRAE Standard. The collector's efficiency and incidence-angle modifier are measured. The test slope and intercept are reported as 0.387 and 0.638, respectively. Garcia *et al.* [1] presented an overview of the parabolic-trough collectors that have been built and marketed during the past century, as well as the prototypes currently under development. A survey of systems which could incorporate this type of concentrating solar system to supply thermal energy up to 400°C, especially steam power cycles for electricity generation, including examples of each application was also reported.

Sagade *et al.* [5] conducted experiments on the prototype parabolic trough made of fiberglass-reinforced plastic with aluminum foil reflector having a reflectivity of 0.86. This line-focusing parabolic trough with mild steel receiver coated with black proxy material has been tested with and without glass cover. Instantaneous efficiency of 51% and 39% has been reported with and without glass cover, respectively.

Several numerical analyses on the PTC with different combinations of boundary conditions, working fluids and concepts were reported in the literature. Reddy and Sathyanarayana [6] numerically analyzed three dimensional models of absorber tubes with porous inserts of different shapes using commercial CFD tools. The performance has been compared for different solar radiation and natural and forced convection heat loss conditions. They reported that the trapezoidal pin receiver with a tip to base ratio of 0.25 showed better performance than other configurations of the order of 13.8% with a relatively lesser pressure drop penalty.

Three dimensional CFD analysis of a PTC has been carried out by using Fluent [7]. In their analysis they have considered the non-linear incident heat flux profile as the thermal boundary condition. The analysis was conducted for the absorber tube where the heat transfer fluid flowed in an annular fashion. Kalogirou [8] developed a detailed thermal model of a parabolic

*Department of Mechanical Engineering, Annamalai University, Annamalai Nagar – 608002, Chidambaram, Tamil Nadu, India.

[+]Chrysler India Automotive Private Limited, Chennai – 600 096, Tamil Nadu, India.

[1]Corresponding author: Tel: +91-75982-22090.
E-mail: akajavali@yahoo.com.

trough collector. The thermal analysis of the collector receiver takes into consideration all modes of heat transfer. The model has been solved using Engineering Equation Solver (EES) and is validated with known performance of an existing collector and the model is found to be satisfactory. Manzolini *et al.* [9] presented a work which deals with the development and testing of an innovative code for the performance prediction of solar trough based concentrated solar power (CSP) plants in off-design conditions implemented in software PATTO.

Shuai *et al.* [10] carried out conjugate heat transfer and thermal stress analyses of tube receiver with concentrated solar irradiation heat flux conditions. A ray-thermal-structural sequential coupled method has been adopted to obtain the concentrated heat flux distributions, temperature distributions and thermal stress fields of tube receiver. The concentrated solar irradiation heat flux distribution converged by solar parabolic collector is obtained by Monte-Carlo ray tracing method and used as boundary conditions for steady state conjugate heat transfer CFD analysis by fitting function method.

The brief review of literature indicated that most of the experimental and numerical studies are focused on conventional PTC designs and limited works has been reported on modified absorber designs. Groenhout *et al.* [11] proposed a novel design for an advanced solar water heater which incorporates a double-sided flat plate absorber mounted on stationary concentrators. Low iron, anti-reflective glass, of the type used in a standard flat plate collector is used for the glass cover and the two concentrating reflectors have been modeled using aluminized reflective sheet. The preliminary results indicate that considerable reductions in heat loss may be obtained with this design compared to conventional designs.

Tao *et al.* [12] presented the operation principle and design method of a new trough solar concentrator. Some important design parameters about the concentrator had been analyzed and optimized. Some characteristic parameters about the concentrator are compared with that of the conventional parabolic trough solar concentrator. It is reported that through the analysis that the new trough solar concentrator can actualize reflection focusing for the sun light using multiple curved surface compound methods. It also has the advantages of improving the work performance and environment of high-temperature solar absorber and enhancing the configuration intensity of the reflection surface.

Zheng *et al.* [13] studied a trough daylight concentration and axial transmission system (TDCAT) based on the previously studied mirror image co-focus concentrator. The TDCAT system concentrates sunlight into a light guide tube where the concentrated sunlight undergoes multi-reflection to be transmitted or eventually absorbed by the media in the tube. The authors hence recommended that the TDCAT system would be suitable for tubular solar bio-reactor or photo catalysis applications.

Li *et al.* [14] conducted experiments and theoretically analyzed a novel Single Pass Evacuated Tube Collector (SPETC) with a symmetrical compound parabolic concentrator (CPC). The novel SPETC is mainly composed of a double-glass evacuated tube deposited the selective absorbing coating, as well as six expansion joints. Also detailed numerical models for thermal behaviors of the SPETC with the CPC reflector, based on the three-dimensional CFD method, have been developed and validated with experimental data. These results suggested that the novel SPETC is feasible for industrial process heat and solar cooling system combined with the adsorption chiller or the desiccant wheel. Another major issue faced by conventional PTC systems is that these systems utilize only the direct radiation and most of the diffused radiation is lost. Even with large volume of work focused towards the PTC by researchers across the world, the efficiency of solar energy conversion is still lower of the order of 25-30%, of the incident solar energy. This indicates that scope exists for improvement in the design of PTC systems to enhance the thermal energy conversion efficiencies.

An attempt was hence made in the present work by modifying the design of the absorber used in the PTC system. The proposed new absorber design consists of an absorber plate and an array of three water tubes attached to the bottom of the plate, running in parallel, to make use of the most of the heat available from the solar energy. Experiments are conducted on both the conventional glazed single tube absorber and the glass sheet covered modified absorber subjected to similar operating conditions. Three dimensional, steady state, conjugate computational fluid dynamic analyses using commercial software Ansys Fluent were conducted for both the single tube and modified absorber design and the results are compared with that of the present experiments. The efficiencies of the conventional single tube absorber and the modified absorber are compared and the results are presented.

2. EXPERIMENTAL SETUP

The construction of the experimental setup used in the present analysis discussed in this section. The trough was fabricated with Fiber Reinforced Plastic (FRP) plate in parabolic shape, following the guidelines of Valan Arasu and Sornakumar [15]. FRP material was preferred since it can withstand wind force and also has extended life. The setup was mounted on a stand which has been fabricated with mild steel angles. The trough was mounted on the support in such way that the trough can be tilted over a wide range of angle which was used for manual sunlight angle tracking. Experiments are conducted between 9.00 AM to 15.30 PM Indian Standard Time (IST) at Annamalai Nagar, India (11.396°N, 79.716°E) with a mean solar beam radiation value ranging from 150 – 850 W/m^2. The mean ambient temperature was 34^{o}C.

2.1 Single Tube Absorber

Figure 1 shows the schematic of the single tube absorber setup on which experiments were conducted with a

specified water flow rate and incident solar heat flux. Copper tube with an outer diameter of 25.4 coated with a non-reflective black paint to absorb heat, was used as the single tube absorber with a d_o/d_i of 1.18. The absorber tube was placed inside an evacuated glass tube of outer diameter 35mm. The parabolic trough reflector was fixed with a focusing light reflector fabricated with mirror strips, fitted over the parabolic trough by applying suitable adhesive. The aperture of the reflector was 1200mm x 1200mm and focal depth D_f was 420mm. Conventionally, the absorber tube axis will be positioned at the focal length of the reflector. Presently, the absorber assembly is fitted above the trough, such that the focused reflected solar beam impinges on the bottom surface of the absorber tube as shown in Figure 1. This can be treated as an off-design condition as any small change in the absorber tube axis distance from the reflector will alter the beam focal point and alters the system efficiency.

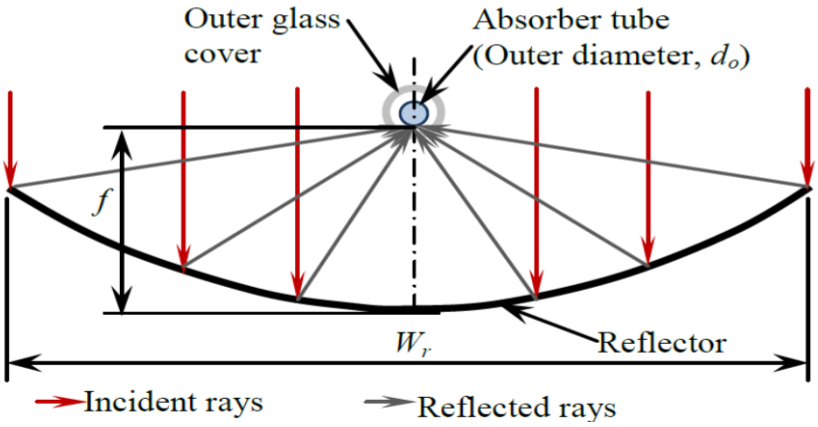

Fig. 1. Arrangement of the PTC with single tube absorber.

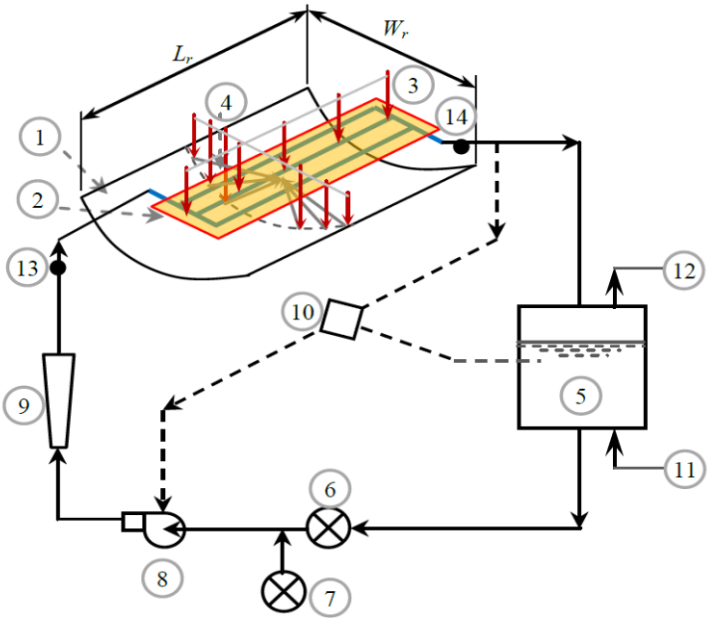

Fig. 2. Schematic of the experimental setup with modified absorber.

2.2 Modified Absorber

The schematic layout of the experimental setup with the modified absorber is shown in Figure 2. The PTC (1) was placed in a stand at an appropriate height convenient for operation and maintenance. A rectangular shaped absorber plate (2) was fabricated, providing a larger surface area for solar rays to impinge on the absorber. The absorber plate was made up of copper plate of 1mm thick and was provided with three numbers of parallel tubes attached to the bottom of the plate. The absorber plate and copper tubes are coated with a non-reflective black paint to absorb heat.

The proposed absorber tube assembly was placed inside a box covered with glass plates in the top and bottom. Water flows inside the tubes connected to a header at the inlet and outlet. Copper tube with outer

diameter of 16 mm was used with a d_o/d_i of 1.14. The diameter of the copper tubes used in the modified absorber was chosen such that the total surface area of the three tubes will be the same as that of the single tube absorber. It was expected that a wider absorber plate increases the quantity of diffused radiation absorbed by the system.

The absorber plate's top surface absorbs the incident radiation (3) (diffuse and direct radiation) whereas the bottom surface of the absorber plate along with the copper tubes absorbs radiation reflected from the parabolic reflector (4). It was expected that due to this combined heating, the efficiency of the proposed modified absorber increases. The length (L_r) and width (W_r) of the reflector are maintained at 1.2m. The hot water thus generated after getting heated up in the absorber system flows to the hot water tank (5). The temperature of the water in the tank was monitored and when it exceeds a temperature of 70^{o}C, the water is pumped out through the outlet connection (12) and fresh cold water was added through the inlet connection (11). A throttle valve (6) was provided at the inlet to control the flow of water flowing through the copper tubes.

When the water temperature is less than the critical temperature, the water by-passes the hot water tank and goes to the pump (8) by using a differential thermostat (10). Any loss in hot water circulating in the system is made up by make-up water (7). The flow rate of water flowing through the modified absorber is measured using a rotameter (9). Water inlet and outlet temperatures, before and after the modified receiver, was measured using two thermocouples; one placed after the rotameter (13) and one at the exit of the absorber (14). The experimental setup shown in the schematic is the complete setup with provision with intermediate hot water storage. However for the present work, open loop type of water circulation was adopted and fresh water was continuously supplied from the make-up water line (7) using the water pump (8). Hence the water inlet temperature was always maintained at the fresh water temperature throughout the experiment.

The geometric details of the modified absorber with plate and tubes are shown in Figure 3(a). Glass covers are fitted at the top and bottom of the absorber plates to utilize the greenhouse effect and the space between the absorber and the glass sheets were evacuated. This helps in trapping the sunlight rays inside the glass cover itself, enabling multiple reflections. As mentioned earlier, the heat flux impinging at the bottom portion of the absorber [10], is considered in the present study, such that the focused beam hits the tube bottom in a small width. The bottom side view of the modified absorber with plate and water tube assembly is shown in Figure 3(b). The absorber assembly is fitted above the trough at the focal line of the parabola, such that the focused reflected solar beam impinges the middle tube bottom surface, as shown in Figure 3(c). Water enters the inlet header and passes through all the three tubes in parallel, joins again at the outlet header before flowing in to the water tank. Figure 4 shows the photograph of the PTC with modified absorber plate assembly. The PTC (1), the modified absorber (2) and the hot water tank (5) are highlighted, taking reference from Figure 1.

J-type thermocouples are fitted on the absorber plate and the glass plate at the top and bottom side. The locations of the thermocouples are shown schematically in Figure 5. The thermocouples on the top side of the absorber plate are shown without braces and that on the bottom side are shown within braces. The outputs of the thermocouples are connected to a display unit from which the temperatures can be noted down directly.

The geometry details of the reflector, modified absorber and the water tubes are detailed below:

- Reflector Length (Lr), Width (W_r): 1.2 [m] both
- Aperture area of the reflector, A_r: 1.44 [m^2]
- Absorber width, W_a: 0.15 [m]
- Copper water pipe diameter ratio (d_o/d_i): 1.14
- Focal distance of the reflector, f : 0.4285 [m]

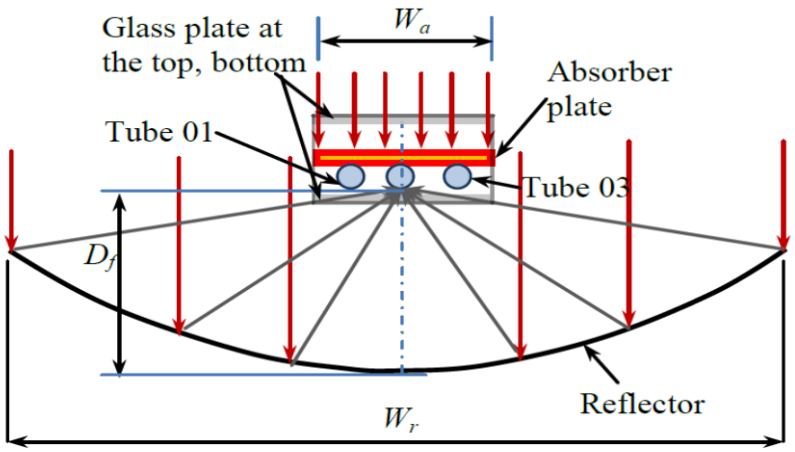

(a) Schematic of the modified absorber.

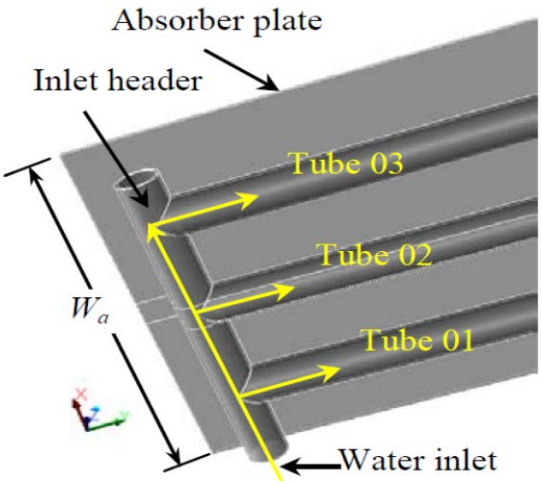

(b) Water flow path in the modified absorber.

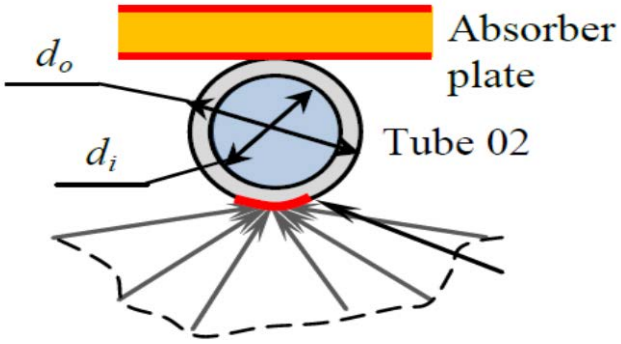

(c) Reflected solar rays incident on bottom of tube 02.

Fig. 3. Details of the incident and reflected solar radiation in the modified absorber.

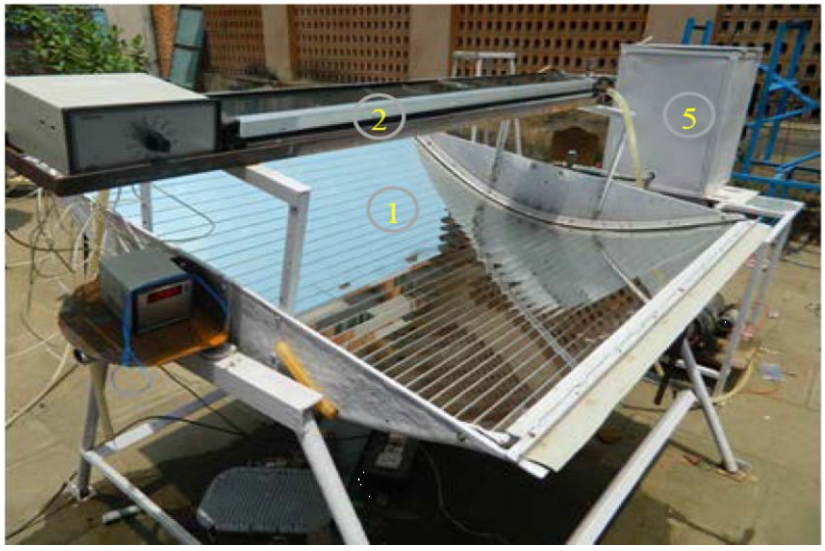

Fig. 4. Photograph of the parabolic trough collector with modified absorber.

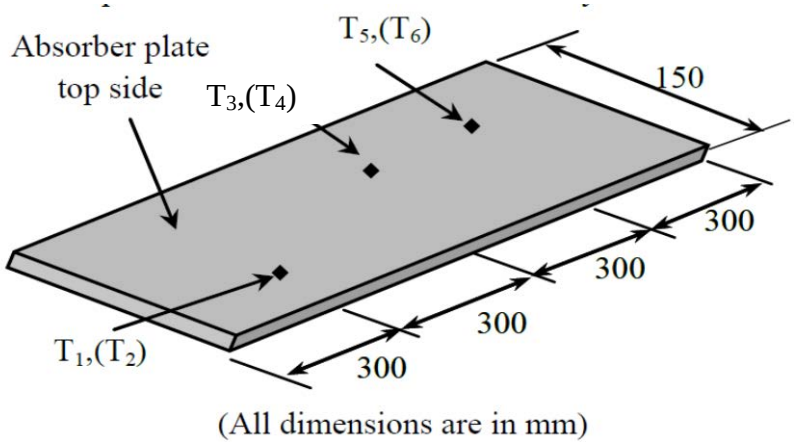

Fig. 5. Details of thermocouples on top and bottom side of the modified absorber.

3. COMPUTATIONAL METHODOLOGY

The fundamental governing equations for flow and heat transfer are the continuity, momentum (Navier-Stokes) and energy equations along with the equations for modeling the turbulence quantities. The governing equations are discussed in detailed in this section. The conservation equations for laminar flow in an inertial (non-accelerating) reference frame are presented here. The equation for conservation of mass, or continuity equation, can be written as follows:

$$\partial\rho/\partial t + \nabla.(\rho\vec{v}) = S_m \quad (1)$$

Equation 1 is the general form of the mass conservation equation and is valid for incompressible as well as compressible flows. The source S_m is the mass added to the continuous phase from the dispersed second phase (e.g., due to vaporization of liquid droplets) and any user-defined sources. The equation for the conservation of momentum in an inertial (non-accelerating) reference frame is given as,

$$\partial/\partial t\,(\rho\vec{v}) + \nabla.(\rho\vec{v}\vec{v}) = -\nabla p + \nabla.(\bar{\bar{\tau}}) + \rho\vec{g} + \vec{F} \quad (2)$$

where p is the static pressure, $\bar{\bar{\tau}}$ is the stress tensor, and $\rho\vec{g}$ and $\vec{F}$ are the gravitational body force and external body forces (e.g., that arise from interaction with the dispersed phase), respectively. $\vec{F}$ also contains other model-dependent source terms such as porous-media and user-defined sources. The stress tensor $\bar{\bar{\tau}}$ is given by

$$\bar{\bar{\tau}} = \mu\left[(\nabla\vec{v} + \nabla\vec{v}^T) - \frac{2}{3}\nabla.\vec{v}I\right] \quad (3)$$

where μ is the molecular viscosity, I is the unit tensor, and the second term on the right hand side is the effect of volume dilation. The CFD code solves the energy equation in the following form, as given in Equation 4 below

$$\partial/\partial t\,(\rho E) + \nabla.\left(\vec{v}(\rho E + p)\right) = \nabla.\left(k_{eff}\nabla T - \sum_j h_j\vec{J}_j + (\bar{\bar{\tau}}_{eff}.\vec{v})\right) + S_h \quad (4)$$

where k_{eff} is the effective conductivity ($k+k_t$), where k_t is the turbulent thermal conductivity, defined according to the turbulence model being used), h is the sensible enthalpy for ideal gases and $\vec{J}_j$ is the diffusion flux of species j. The first three terms on the right-hand side of the equation represent energy transfer due to conduction, species diffusion, and viscous dissipation, respectively.

From the principle of conservation of energy, the energy absorbed by the sink in a system is the energy that is transferred from the source. It is thus clear that the entire energy incident on any system need not be absorbed or transferred by the system. Following this, for the present CFD analysis, the total heat incident on the bottom of the absorber tube or modified absorber is estimated from the experimental heat gained by the coolant fluid in the system. Thus the experimental efficiency of the system under consideration is helping in identifying the heat input for the numerical analysis.

3.1 Computational Domain – Single Tube Absorber

Figure 6(a) shows the computational domain of the single tube absorber used for the present CFD analysis. A focused heat flux region is specified at the tube outer surface of the single tube absorber by creating a split on the bottom side of tube outer surface. The width of the focused region where the heat flux impinges is fixed at 5 mm for the present study. This value is notional as the exact width of the beam impinging on the bottom mid tube in the experiments is not measurable, due to difficulty in access.

Meshing is carried out in a conjugate fashion using Gambit 2.4 pre-processing to generate hexahedral elements throughout the computational domain as in Figure 6(b). Finer near wall meshing is developed using the boundary layer mesh feature of the pre-processor with the first node at 0.1mm and with a default growth factor of 1.1 for 10 layers. This is done to capture the flow features close to the wall more accurately.

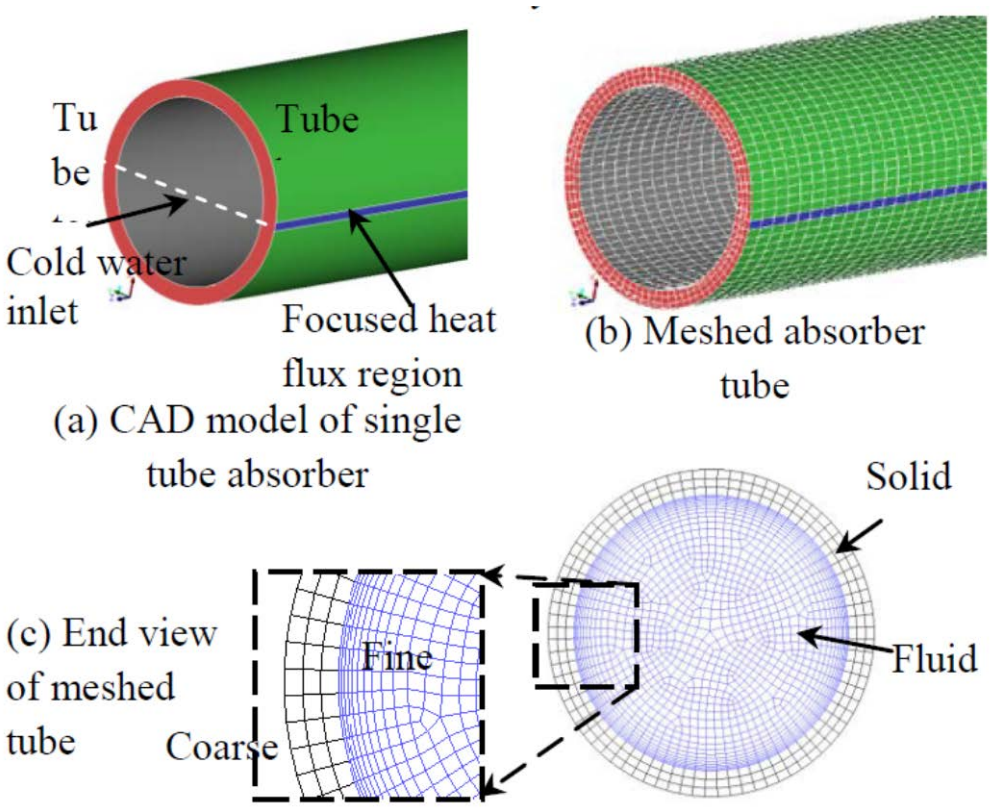

Fig. 6. Computational domain of single tube absorber - (0.97 Million cells).

Grid independency tests are carried out for the single tube absorber taking the surface averaged fluid outlet temperature as the assessment criteria. Three meshes were generated with three different mesh sizes to form coarse, medium and fine meshes with 0.65, 0.97 and 1.3 million cells respectively.

Figure 7 shows the variation of fluid outlet temperature on computations with different mesh densities. It was observed that the temperature value increases from a mesh size of 0.65 to 0.97 million. But the variation of this value from 0.97 to 1.3 million cells is very less, which indicates that the effect of mesh density is insignificant beyond 0.97 million cells and hence it was decided to continue with the mesh settings of 0.97 million cells for the present study. The end view of the computational mesh with 0.97 million cells along with finer near inner wall is shown in Figure 6(c).

3.2 Computational Domain – Modified Tube Absorber

The water carrying copper tubes that are attached to the modified absorber plate forms the computational domain of present study. Water is passed through the copper tubes and carries the heat gained by the absorber system. Figure 8(a) shows the isometric top view of the domain whereas Figure 8(b) shows the isometric bottom view of the modified absorber where green region indicates the area over which the appropriate value of heat from the experiments was specified as a constant heat flux boundary condition.

The heat flux impinging at the bottom portion of the absorber, similar to [10] is considered in the present study, such that the focused beam hits the tube bottom in a small width. To avoid any possible mesh issue due to sharp corner and line contact, the tube geometry is made to merge with the plate to have an area contact. The mesh for the computational domain of the modified absorber was developed similar to that of the single tube absorber where hybrid meshing, a combination of tetrahedral and hexahedral cells was employed. The straight tube regions and most of the absorber plate regions are meshed with unstructured hexahedral elements whereas the more complex regions like pipes intersection are meshed with tetrahedral elements.

3.3 Boundary Conditions – for both Single Tube and Modified Absorber

The boundary conditions used for the present conjugate thermal computational fluid dynamic analyses are taken from the present experiments. The water flow rate has been set at 18 kg/hr for both the single tube and modified absorber tube systems, with a mass flow inlet boundary condition at the computational domain inlet. As discussed earlier the water flow is supplied from the makeup water line throughout the experiment and the water inlet temperature is set at 32^{o}C.

Based on the experimental energy balance between (a) the total heat incident on the absorber system and (b) the heat carried by the coolant water at the outlet, an appropriate heat flux value taken for the CFD analysis. A static pressure value of ‘zero’ indicating the water flows out to atmosphere is specified at the outlet boundary of the computational domain. Heat loss by convection from the air exposed tube surfaces and

bottom side of the modified absorber is specified with a constant value of heat transfer coefficient. Thermal energy loss due to radiative heat transfer has not been considered in the present analysis. Based on the mass flow rate and tube dimensions, the calculated Reynolds numbers are found to fall well below the critical value and hence the flow is treated as laminar in the present computations.

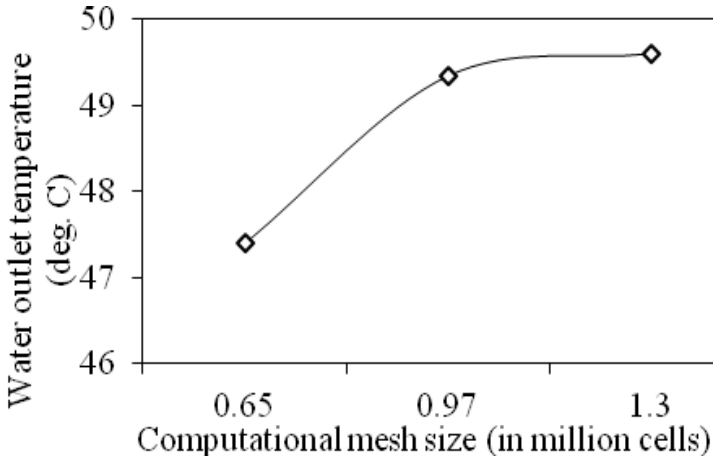

Fig. 7. Water outlet temperature at different grid sizes – Single pipe.

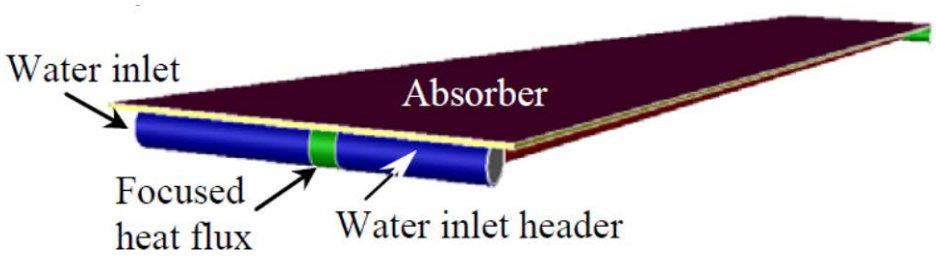

(a) Isometric top view.

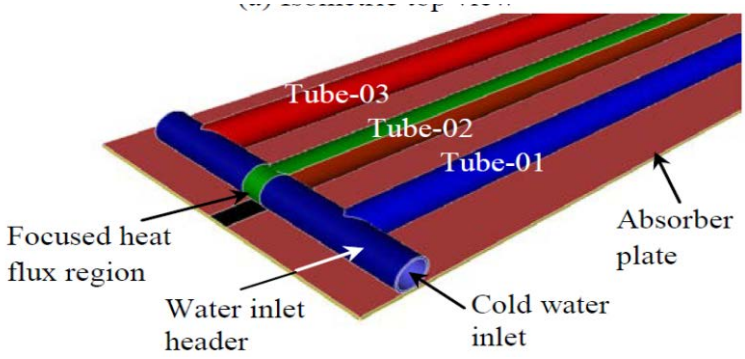

(b) Isometric bottom view.

Fig. 8. Computational model of the modified absorber system with copper plate and three water pipes.

3.4 Data Reduction

The flow Reynolds number is estimated based on the specified inlet mass flow rate and pipe inlet hydraulic diameter and properties of water at its inlet temperature. The Reynolds number is estimated as,

$$\mathrm{Re} = 4.\dot{m}/\rho\mu D_h \quad (5)$$

The solar irradiance is measured using a Pyranometer, which is an instrument for direct measurement of solar irradiance. Sunlight enters the instrument and is directed to a thermopile which converts heat to an electrical signal. The signal voltage is converted using a formula to estimate the solar intensity, q_{in}".Not all the heat energy incident is reflected by the concave reflector as some portion of the energy is dissipated. From standard texts this value is identified as 20%. Also the area of the modified absorber plate (A_{abs}) blocks the sunlight from directly

hitting the reflector and this portion of the reflector area (A_{ref}) is not useful. Thus the net heat incident on the absorber system, Q_{in}(Watts) is estimated as

$$Q_{in} = 0.8.(A_{ref} - A_{abs}).q_{in}'' \quad (6)$$

The heat gained by water, Q_w (Watts), flowing through the solar water heating system is estimated by measuring the by using the formula,

$$Q_w = m.C_p.(T_{w,out} - T_{w,in}) \quad (7)$$

The efficiency of the absorber system, η_{abs} (%), is estimated as a percentage of heat gained by water from the heat that is incident on the absorber system.

$$\eta_{abs} = Q_w/Q_{in} \quad (8)$$

3.5 *Convergence Criteria*

The convergence criteria for the computational solution are determined based on scaled residuals for the equations of continuity, momentum equations and turbulence quantities specific to the respective models. The scaled residuals for solution convergence are set to 10^{-5} for all governing equations and turbulence quantities. The solution is considered to be converged when all the scaled residuals are less than or equal to this prescribed value. Computations are carried out until the steady state is reached. For few cases, the convergence is not achieved to the desired accuracy. In those cases, the iteration is continued further to a stage that the results do not vary even after 500 iterations, thus achieving iterative convergence.

4. RESULTS AND DISCUSSIONS

4.1 *Single Tube Absorber - STA*

Experiments are carried out on the single tube absorber (STA) with a water flow rate of 18 kg/hr and inlet temperature of 32°C water inlet and outlet temperature were measured at 30 minute intervals. The water inlet and outlet temperatures were used to estimate the heat gained by water. Computations are carried out on the single tube absorber domain for heat input of 839.4 W corresponding to 10.30 AM, which is 744 W/m^2. The heat input is specified in the form of constant heat flux, with the flux value estimated by using the area of the small focused heat flux concentration area at the bottom of the single tube absorber as in Figure 1.

Comparison of water outlet temperature between experimental value and CFD results for the single tube absorber, for the 10:30 AM data, with 32°C water inlet temperature is shown in Figure 9(a) and the results for the peak water outlet temperature is plotted in Figure 9(b). This shows good agreement between experiment and CFD.

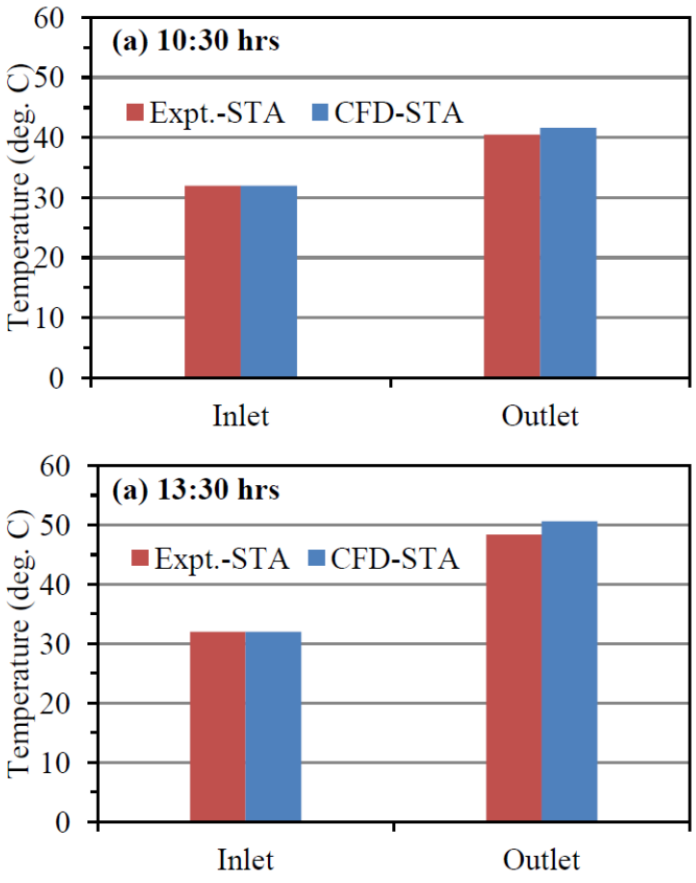

Fig. 9. Comparison of water temperatures between experiments and CFD for the single tube absorber.

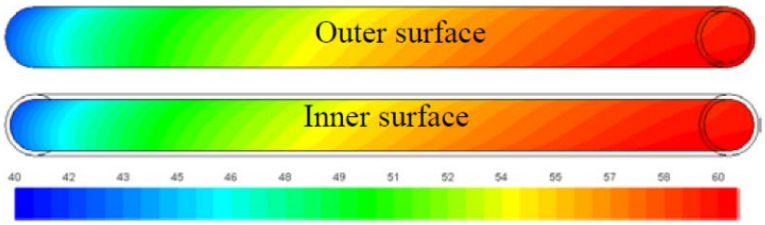

Fig. 10. Wall temperature distribution at tube surface (deg. C) - Single tube – 10:30 AM data.

The experimental water outlet temperature at 10:30 AM was found to be 40.5°C, whereas in the CFD it was 41.6°C. A difference in water outlet temperature of 1.1°C was observed between the present computations and the present experiments, with the CFD results larger than the experiments. This accounts for a difference of 2.7% and may be due to the fact that the computations did not considered the heat loss from the relatively hot absorber tube to the surroundings. Also it is to be noted that the glass envelope and vacuum space surrounding the absorber tube was not considered in the computations. Considering the fact that the PTC presently tested is a prototype model with aperture area of 1.44m^2, the peak outlet temperature on the test day was found to be 50.2°C.

Figure 10 shows the wall temperature distribution at tube outer and inner surface which shows the temperature patterns which are formed due to the heat input at the bottom of the tube. It can be inferred from this plot that the peak inner wall temperature is observed at the bottom of the tube. It can also be observed that the minimum and maximum temperature values increase with the axial distance from the inlet.

4.2 Modified Absorber –Header Tube Absorber - HTA

Experiments are conducted on the modified absorber (HTA) at a water flow rate of 18 kg/hr, with an inlet temperature of 32°C, for a total duration of 5 hours during the day. It is normally used with a solar tracking system to keep the instrument aimed at the sun. Data are extracted at the various thermocouple locations in water inlet, outlet and absorber plate temperatures at various locations and glass plate temperatures and recorded. The temperatures one each at the top and bottom glass plates is also recorded. Computations are performed for the 10.30 AM data with 23.4% absorber efficiency, for the purpose of validating the present computational results for the modified absorber geometry. Heat input for this case is estimated from the heat gained by water and this heat value is specified on the focused heat flux region.

Figure 11 shows the contours of wall temperature distribution on the modified absorber plate, tubes and headers. The temperature contours on the top side of the absorber plate is shown in Figure 11(a) whereas the temperature values on the tubes and bottom side of the absorber plate is shown in Figure 11(b). The wall temperatures in the domain is in the range of 40 to 73 deg. C, where low temperatures are observed close to the water inlet and temperature increase in stream wise direction.

Among the three parallel tubes, the middle tube (Tube 02) shows the highest outer wall temperature since the heat flux input is specified in this tube. A unique pattern of wall temperature is observed from the computational results. Non uniform temperature contours between the tubes indicate that the flow distribution is not uniform across the tubes. Low temperatures (blue regions) in the region near inlet header show the partially filled pipes due to the 90 degree turning between inlet header and the three parallel tubes. Reaching the outlet header region, the water flowing inside the tube assembly gets heated up and comes out at a higher temperature. The fluid from the three parallel tubes mixes at the outlet header and vents out of the system.

Figure 12 shows the comparison of inlet and outlet water temperature between the present CFD and experiments. The experimental water outlet temperature at 10:30 AM for the single tube absorber was found to be 40.5°C, whereas in the CFD it was 41.6°C. The different in water outlet temperature of 1.1°C was observed between the present computations and the present experiments. The computational water temperature at the outlet is 2.7% higher than its experimental counterpart. Similar value for the modified absorber was found to be 4.1%. It can be observed that the agreement between the present CFD and present experiments is excellent which vindicates that the presently adopted computational methodology.

Figure 13 shows the comparison of efficiency of the absorber estimated from the experimental data measured. Heat gained by the absorber tube is found to increase with time from the start of the experiment and the percentage of heat gained by the STA range from 9% to 39%, whereas the HTA this value was found to vary from 23% to 56%. The day average collector efficiency by STA was estimated as 26.8%, whereas the modified absorber showed 42.2%. These numbers indicate that the proposed modified absorber systems is certainly efficient than the conventional glass enveloped single tube absorber typically used in the solar energy recovery systems. Figure 13 also shows the solar intensity values (in W/m^2) measured during the experiments conducted with the modified absorber.

The peak efficiency for the single tube absorber was observed to be close to 40% at 13:30 hrs whereas for the modified absorber it was observed to be close to 56% at around 14.00 hrs. In the modified absorber, the

efficiency of the absorber was found to continue in this range for more than an hour and drops at 15.30 hrs. Higher efficiencies in the modified absorber can be attributed to the increased surface area in the modified absorber, which enables trapping of more direct and reflected heat from the solar rays. This helps in increasing the efficiency of the modified absorber. Small errors in off focal targeting of rays and tracking errors will be taken care by increased absorber width.

It can thus be concluded that the proposed modified absorber design in found to perform better in terms of increased solar energy absorption and hence recommended for use in solar parabolic trough collectors. It will be an interested area of research to do further modification in the modified absorber to optimize the design and operating parameters.

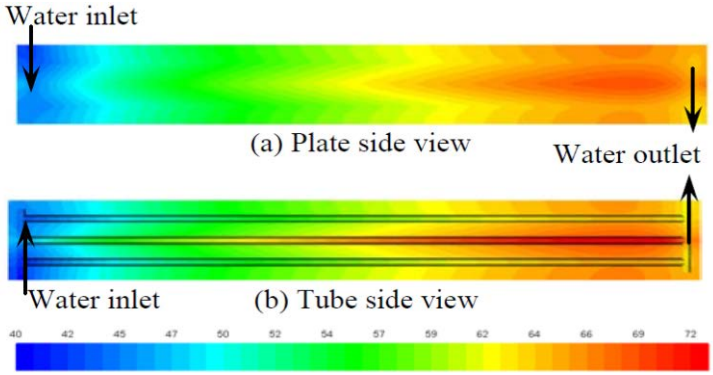

Fig. 11. Contours of wall temperature distribution (°C) on the modified absorber – 10:30 AM data.

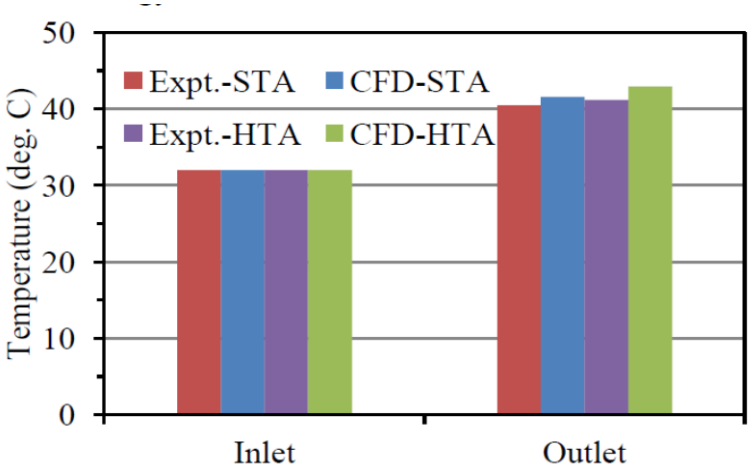

Fig. 12. Comparison of water temperature from present experiments vs. computation – 10:30AM data.

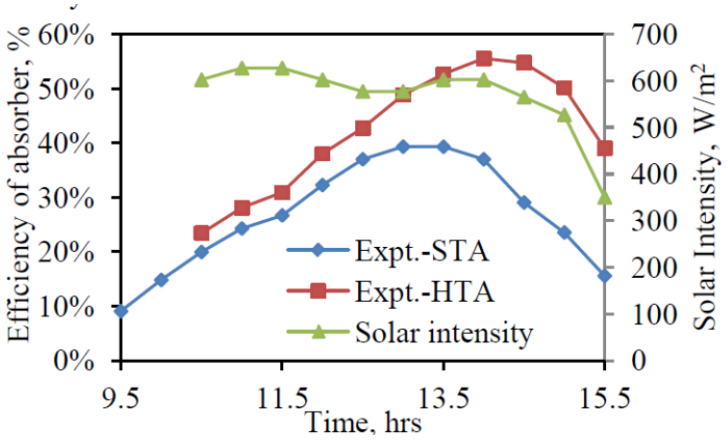

Fig. 13. Comparison of absorber efficiency with time.

5. CONCLUSION

Experiments and numerical computations are conducted on a single tube absorber and a modified absorber where a plate and an array of three water tubes are used to extract the heat absorbed from the direct and diffused solar radiation. Three dimensional, conjugate thermal computational fluid dynamic analyses using a commercial code Ansys Fluent was conducted both for the single tube absorber and the modified absorber design. The present computational results showed good agreement with that of the present experimental results. Numerical analysis conducted on single tube absorber showed a lesser solar energy recovery than the modified absorber.

The solar energy recovery is improved with the modified absorber design, in the form of increased water temperature, thus increasing the efficiency of the absorber. From the experimental data, it was found that the day average collector efficiency of the modified absorber was 42.1% which was higher than the conventional single tube absorber whose value was 26.7%.

REFERENCES

[1] Fernandez-Garcia A., Zarza E., Valenzuela L. and Perez M., 2010. Parabolic-trough solar collectors and their applications. *Renewable and Sustainable Energy Reviews* 14: 1695–1721.

[2] Ericsson J., 1884. The sun motor and the Sun's temperature. *Nature* 29: 217–219.

[3] Spencer L.C., 1989. A comprehensive review of small solar-powered heat engines: Part I. A history of solar-powered devices up to 1950. *Solar Energy* 43(4): 197–214.

[4] Kalogirou S., 1996. Parabolic trough collector system for low temperature steam generation: design and performance characteristics. *Applied Energy* 55(1): 1-19.

[5] Sagade A.A., Aher S. and Shinde N.N., 2013. Performance evaluation of low-cost FRP parabolic trough reflector with mild steel receiver. *International Journal of Energy and Environmental Engineering* 4(5): 1-8.

[6] Reddy K.S. and G.V. Sathyanarayana. 2008. Numerical study of porous finned receiver for solar parabolic trough concentrator. *Engineering Applications of Computational Fluid Mechanics* 2(2): 172-184.

[7] Islam M., Karim A., Saha S.C., Miller S. and Yarlagadda P.K.D.V., 2012. Three dimensional simulation of a parabolic trough concentrator thermal collector. In *Proceedings of the 50th Annual Conference*, Australian Solar Energy Society (Australian Solar Council) Melbourne, ISBN: 978-0-646-90071-1

[8] Kalogirou S.A., 2012. A detailed thermal model of a parabolic trough collector receiver. *Energy* 48: 298-306.

[9] Manzolini G., Giostri A., Saccilotto C., Silva P. and Macchi E., 2011. A numerical model for off-design performance prediction of parabolic trough based solar power plants. *Journal of Solar Energy Engineering* 134(1): 011003 (10 pages).

[10] Shuai Y., Wang F.-Q., Xia X.-L. and Tan H.-P., 2010. Ray-thermal-structural coupled analysis of parabolic trough solar collector system. In *Solar Collectors and Panels, Theory and Applications*, Dr. Reccab Manyal, ed. ISBN: 978-953-307-142-8, InTech, DOI: 10.5772/10344.

[11] Groenhout N.K., Behnia M. and Morrison G.L., 2002. Experimental measurement of heat loss in an advanced solar collector. *Experimental Thermal and Fluid Science* 26: 131–137.

[12] Tao T., Hongfei Z., Kaiyan H. and Mayere A.K., 2011. A new trough solar concentrator and its performance analysis. *Solar Energy* 85(1): 198–207.

[13] Zheng H., Feng C., Su Y., Wang R. and Xue X., 2013. Performance analysis and experimental investigation of a novel trough daylight concentration and axial transmission system. *Solar Energy* 97: 200–207.

[14] Li X., Dai Y.J., Li Y. and Wang R.Z., 2013. Performance investigation on a novel single-pass evacuated tube with a symmetrical compound parabolic concentrator. *Solar Energy* 98(C):275–289.

[15] Valan Arasu A. and T. Sornakumar. 2007. Design, manufacture and testing of fiberglass reinforced parabola trough for parabolic trough solar collectors. *Solar Energy* 81: 1273–1279.